Biomed Microdevices (2007) 9:877–883
DOI 10.1007/s10544-007-9101-3

Electrical capture and lysis of vaccinia virus particles using silicon nano-scale probe array

Kidong Park · Demir Akin · Rashid Bashir

Published online: 3 July 2007

Abstract A probe array with nano-scale tips, integrated into a micro-fluidic channel was developed for the capture and lysing of small number of vaccinia virus particles using dielectrophoresis. The nano-scale probe array was fabricated in Silicon on Insulator (SOI) wafers, and sharpened with repeated oxidation steps. The gap between each probe ranged from 100 nm to 1.5 μm depending on fabrication parameters. The probe array was used to capture vaccinia virus using positive dielectrophoresis (DEP) from a flow within the microfluidic channel, and then the same probe array was used to apply high electric field to lyse the virus particles. It was shown that under electric field strengths of about 10^7 V/m, the permeability of ethidium bromide into the vaccinia virus particles was increased. Upon SEM analysis, the particles were found to be damaged and exhibited tubules networks, indicating disintegration of the virus outer layer. In addition, elongated strands of DNA were clearly observed on the chip surface after the application of the high electric field, demonstrating the possibility of electrical lysis of virus particles.

K. Park · D. Akin · R. Bashir
Birck Nanotechnology Center, Purdue University,
West Lafayette, IN 47907, USA

K. Park · R. Bashir
School of Electrical and Computer Engineering,
Purdue University,
West Lafayette, IN 47907, USA

D. Akin · R. Bashir (✉)
Weldon School of Biomedical Engineering, Purdue University,
West Lafayette, IN 47907, USA
e-mail: bashir@purdue.edu

Keywords Dielectrophoresis (DEP) · Electrical lysis · Vaccinia virus · Micro-fluidic chip

1 Introduction

Sample preparation is a critical module in a miniaturized and integrated biological and chemical analysis system. Especially, for analysis of intracellular material, the system should be able to lyse the particle and extract the target molecule undamaged and pure. Moreover, the lysis module should be seamlessly integrated into the overall system. The lysis methods can be generally divided into reagent-assisted or reagent-less lysis methods. The former uses lytic agents such as detergent to lyse cells. However, these lytic reagents can interfere following analysis process and the system can be overly complicated due to lytic agent injection and sample rinsing step.

Therefore, reagentless lysis methods integrated into the microfluidic platform have been developed with various approaches. Those reagentless lysis methods can be largely categorized as mechanical (Carlo et al. 2003), thermal (Lie et al. 2004; Waters et al. 1998), and electrical (Lee and Tai 1999; Lu et al. 2005; Lee and Cho 2006; Wang et al. 2006). The mechanical methods utilize sharp structure to damage the particle's membrane and extract the intracellular material. However, in mechanical lysis methods, the size of the sharp structures should be decreased as the sample size decreases. Moreover, the fabrication process can be challenging, and costly. The thermal lysis methods are using high temperature (~94°C) to lyse the cell, but the thermal lysis methods are not suitable for the heat sensitive molecule, such as protein.

The electrical lysis methods are usually based on the irreversible electroporation of the lipid bilayer of the target

particles. Externally applied electric filed produces the transmembrane potential, and it generates electric field inside the lipid bilayer membrane. This internal electric field generates a Maxwell stress, $\frac{1}{2}\varepsilon E^2$, compressing the membrane in the normal direction, and rupture the membrane if the electric field is above critical value (Lewis 2003). External electric filed can be generated via electrode itself (Lee and Tai 1999; Lu et al. 2005), or it can be generated by the decreased cross-section of the conducting fluid (Lee and Cho 2006; Wang et al. 2006), similar to the electrodeless dielectrophoresis (Chou and Zenhausern 2003). However, above approaches are mostly targeted for mammalian cells and bacteria.

The electrical lysis of viruses has not been reported, especially in micro fluidic environment. As the size of the particle is decreased, a stronger electric field is required to produce enough transmembrane potential across the lipid bilayer to lyse the particle. To the best of our knowledge, only the dielectrophoresis (DEP) capture, the measurement of the dielectric characteristic (Hughes et al. 2002; Hughes and Morgan 1998; Grom et al. 2006) and chemical lysis of Cymbidium mosaic virus (Yobas et al. 2005) have been reported in literature, but the electrical lysis or electroporation of virus particles has not been tried yet. In an earlier report, we used planar interdigitated electrodes in a microfluidic channel and used DEP to capture and image virus particles in real time (Akin et al. 2004).

In the current paper, a nano scale probe array was developed for DEP capture and reagentless lysis of the vaccinia virus. The probe array was integrated with polydimethylsiloxane (PDMS) microfluidic channel to provide optical observation as well as safe sample handling. The nano-scale probe array was fabricated in a SOI (silicon-on-insulator) wafer and released from the substrate to form a 3-dimensional structure to produce spatially localized electric field. The virus particles were first

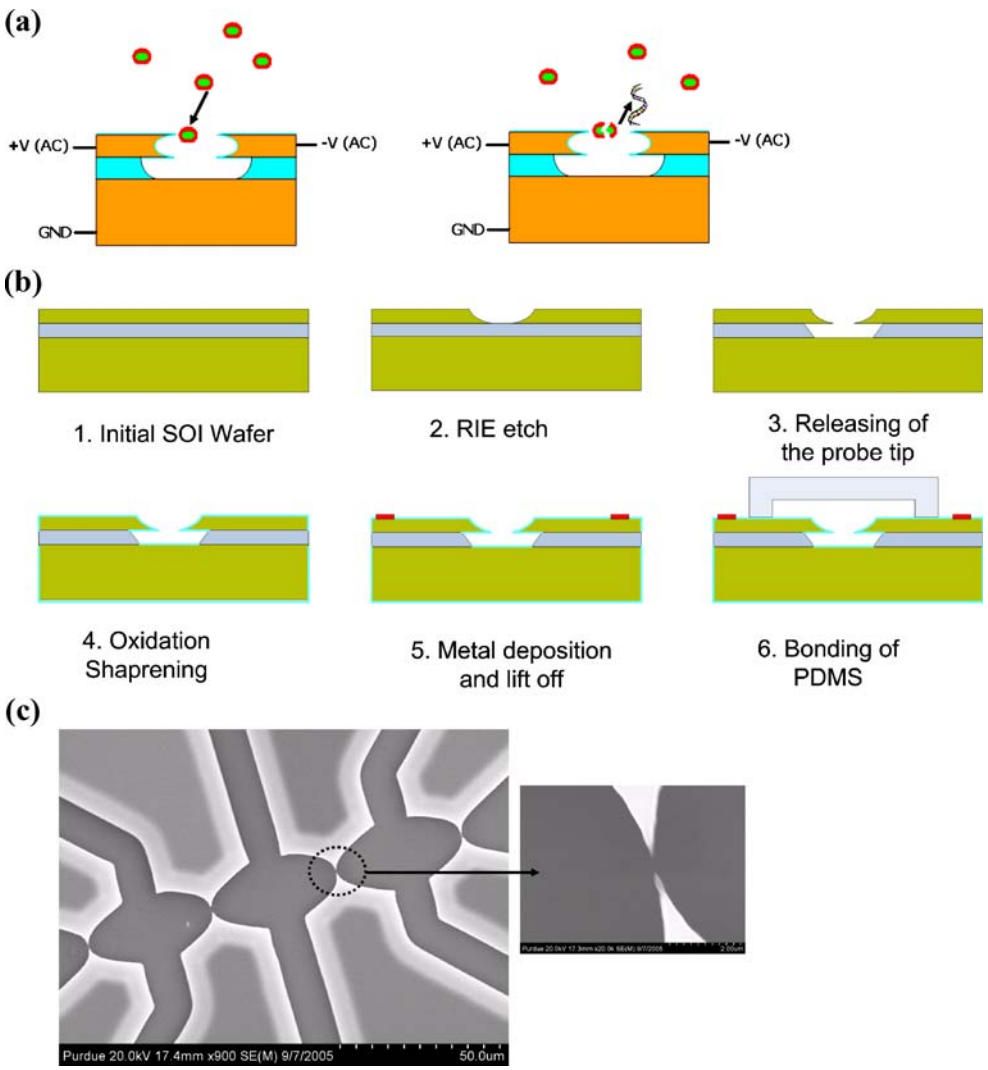

Fig. 1 (**a**) Capture and lysis of the vaccinia virus, (**b**) Schematic diagram of the fabrication process. (**c**) SEM images of the fabricated devices

Table 1 The dielectric characteristic of the vaccinia virus from fitting of our experimental data, and that of the Herpes virus from the literature (Hughes et al. 2002)

	Membrane conductivity (δ_{mem})	Membrane relative permittivity (ε_{mem})	Bulk conductivity (δ_{mem})	Bulk relative permittivity (ε_{mem})
Herpes simplex virus type 1	0.3±0.1 nS	7.5±1.5	100±5 mS/m	75±25
Vaccinia virus	0.19 nS	10.3	160 mS/m	65

attracted to the probe array and then were electrically lysed, as schematically shown in Fig. 1(a). The use of nano-scale probes allows the capture of very few virus particles. Fluorescence microscopy and scanning electron microscopy (SEM) were used to prove the capture and the lysis of the virus.

2 Experimental section

Device fabrication The starting material was a highly doped SOI wafer, with a 2 μm thick device layer and a 2 μm thick buried oxide layer. The fabrication flow is shown in Fig. 1(b). First, the shape of the probe array was formed on the device layer with isotropic reactive ion etching (RIE). The formation of the probes with isotropic plasma etching are more finely tunable to produce a range of gap between probes than the previously reported method (Bourland et al. 2001). The buried oxide layer was etched and, the released probe array was further sharpened by repeated oxidation and oxide etching steps (Ravi et al. 1991). Then, a metal layer (Au/Ti) was deposited and patterned for the wire bonding pad. Figure 1(c) shows the SEM image of a probe array on a die after oxidation sharpening. The gap between each probe ranged from 100 nm to 1.5 μm depending on fabrication parameters. With the fabricated probe array, high electric field about 10^7 V/m can be easily achieved with regular function generators.

The fabricated silicon chip was attached to a printed circuit board (PCB) for electrical connections and a PDMS cover with channel was attached to the chip. Each probe in the probe array had individual electrical access through the PCB. The dimension of the channel was 7 μm high, 2,500 μm wide, and about 1.5 mm long, considering the fluid velocity, the internal pressure, and capture efficiency.

Sample preparation and imaging Vaccinia virus (Western Reserve strain) was used in our studies. Vaccinia virus is an enveloped DNA virus, with a genome of 200 kb. Mature virus is rounded brick shaped and has a dimension of about 360×270×250 nm (Cyrklaff et al. 2005). It is a membraned particle containing a biconcave core, containing DNA. The internal structure of the vaccinia virus is not yet completely known, but the most probable theory up to date is the single membrane bilayer model, in which the whole particle is surrounded by a single lipid bilayer, and the core and DNA is not surrounded by the lipid bilayer (Condit et al. 2006).

The initial viral concentration was 9×10^{12} pfu/ml. The sample was diluted 10^{-2} times, and then inactivated with ultraviolet light. The sample was then filtered through a 0.4 μm pore-size membrane filter to remove aggregated virus particle and possible impurities. For capture experiment, the virus particle was dual labeled with trihydrochloride, trihydrate (Hoescht 33342 dye, Molecular Probes, Eugene, OR) and 3,39-dihexyloxacarbocyanine iodide ($DiOC_6(3)$ dye, Molecular Probes). The former is a blue-fluorescent cell-permeable DNA counterstain dye and the latter is a cell-permeable green-fluorescent lipophilic dye. Each dye will simultaneously stain the outer lipid bilayer and the DNA (Akin et al. 2004; Ghafoor et al. 2006). The 100 μl of filtered sample was mixed with 1 μl of $DiOC_6(3)$ and 4 μl of Hoescht 33342, and incubated for 30 min. After incubation, the sample was ten times diluted and used for the experiment. The final concentration for the capture experiment was 9×10^9 pfu/ml.

For the lysis experiment, ethidium bromide was used as a fluorescent dye. Ethidium bromide is a red fluorescent dye for DNA, which can not penetrate the lipid membrane. The final concentration was 9×10^{10} pfu/ml and the final concentration of the ethidium bromide was 2 μg/ml. The

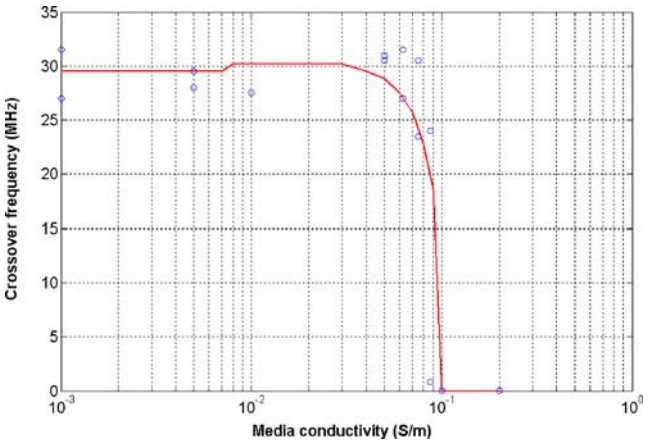

Fig. 2 The measured cross-over frequency of the vaccinia virus and the fitted curve. The *solid line* shows the fitted curve, with aid of the multi-shell model

sample was used after 30 min incubation. For the measurement of the crossover frequency, the vaccinia virus was stained only with $DiOC_6(3)$ with same concentration, and the conductivity was adjusted with the sodium chloride solution. A fluorescent microscope (Nikon Eclipse E600FN, Japan) was used for capturing fluorescent images. To capture the fluorescent image of the dual-labeled particle, two different images were taken for each fluorescent filter successively, and then the two images were digitally superimposed with each other and then digitally enhanced for clarity.

After the capture and lysis experiment, the chip surface was observed with SEM. PDMS cover was carefully removed with the DEP voltages turned on and the device

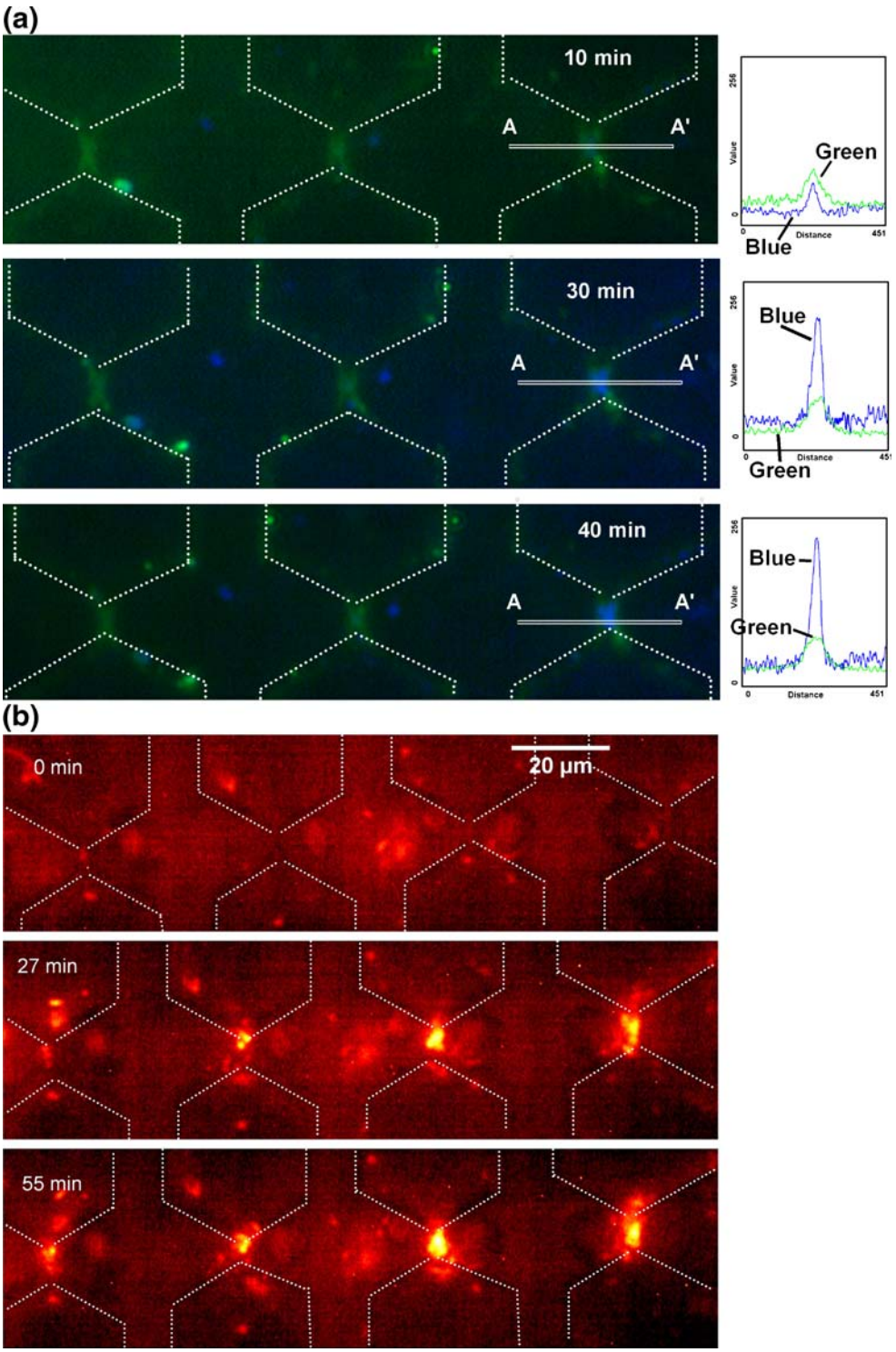

Fig. 3 (**a**) The progression of the vaccinia virus capture at 10, 30 and 40 min. The intensity of the fluorescence from Hoescht 33342 and $DiOC_6(3)$ are plotted at each time point. (**b**) The progression of the capture of the vaccinia virus, stained with ethidium bromide

was dried in air by keeping it in a sterile box overnight at room temperature. The device surface was imaged by Hitachi s4800 FESEM microscope (Tokyo, Japan).

3 Results and discussion

Measurement of the dielectrophoresis crossover frequency To estimate the Clausius-Mossotti factor of the vaccinia virus, the crossover frequency of the vaccinia virus was measured, in similar way as reported earlier (Hughes et al. 2002). The sample was loaded on the interdigitated electrodes, with 23 μm wide electrode, and 17 μm gap. The electrodes were excited with 20 Vpp AC signal and the movement of the vaccinia particle was observed with a fluorescence microscope. By observing the movement of the particle while changing the frequency, the transition between the positive and negative dielectrophoresis was determined, and the crossover frequency was recorded.

The internal structure of the virus particle was assumed to be the single membrane bilayer model (Condit et al. 2006) and the virus was modeled with a multi-shell model (Chan et al. 1997), having an insulating lipid bilayer membrane, and the conductive internal materials. The following equation shows the particle's complex permittivity, where ξ_{in}, and ξ_{mem} are complex permittivity of the internal material and the membrane.

$$\xi_p = \xi_{mem}\frac{\left(\frac{R}{r}\right)^3 + 2\left(\frac{\xi_{in}-\xi_{mem}}{\xi_{in}+2\xi_{mem}}\right)}{\left(\frac{R}{r}\right)^3 - \left(\frac{\xi_{in}-\xi_{mem}}{\xi_{in}+2\xi_{mem}}\right)}$$
$$\text{where, } \xi_{in} = \varepsilon_{in} - j\delta_{in}/(2\pi^* f), \xi_{mem} = \varepsilon_{mem} - j\delta_{mem}/(2\pi^* f) \quad (1)$$

The measured crossover frequency was fitted to find the optimum value of the permittivity and the conductivity of each part as shown in Table 1, with comparison to the values of herpes virus (Hughes et al. 2002). Figure 2 presents the measured crossover frequency and a fitted curve.

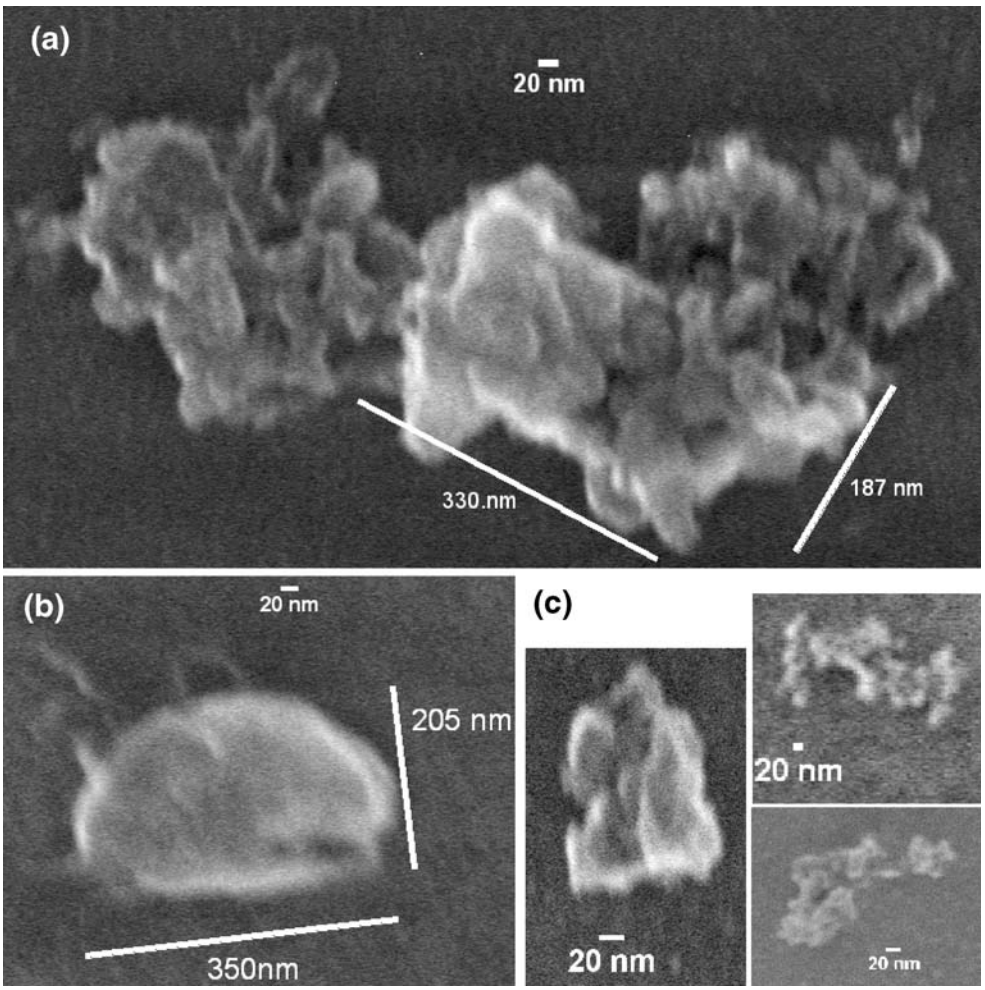

Fig. 4 (**a**) SEM images from our chips showing a vaccinia virus particle. (**b**) The fully lysed virus particle. (**c**) Fragment of the tubules, found on the device surfaces

Capture of vaccinia virus The vaccinia virus was captured by positive DEP with a nano scale probe array. The fluid velocity was 0.1 mm/s and the two sinusoidal DEP signals with 180° phase difference were applied to each pair of the probe. The amplitude was 20 Vpp and the frequency was 100 kHz.

Figure 3(a) shows the progression of the capture after 10, 30 and 40 min from the initial application of DEP voltage. At 10 min after the initial application of DEP voltage, the captured vaccinia virus particles were found between each probe, and the mixture of green and blue can be observed. At 30 and 40 min, increased number of the captured particles was observed as expected.

In Fig. 3(a), the strength of the fluorescence is plotted along the line A-A'. The green line is the intensity of the $DiOC_6(3)$, coming from the lipid bilayer of the vaccinia virus, where as the blue line is the intensity of the Hoescht 33342 from the viral DNA. As can be seen in the plot, the peaks of the each fluorescent signals are colocalized to each other, indicating the captured particles are the vaccinia virus.

Lysis experiment of vaccinia virus For clearer proof of the lysis of the vaccinia virus, ethidium bromide was used in the lysis experiment. Ethidium bromide was chosen as a fluorescent dye, since it can't penetrate through the intact lipid bilayer membrane of the vaccinia virus, where as it can stain the exposed DNA.

Prior to the injection into the device, the vaccinia virus sample was thoroughly observed to confirm that there were no particles stained with ethidium bromide. The sample was injected into the device with the average fluid velocity of 0.1 mm/s. The dielectrophoresis signal of 20 Vpp at 100 kHz was applied, after the device was filled with sample. Figure 3(b) presents the progression of the capture and lysis of the vaccinia virus, at 0, 27 and 55 min after initial application of the DEP voltages and sample injection. The strong fluorescence signal came only from the probe area, where the highest electric field was produced. Therefore the strong electrical field damaged the vaccinia virus membrane, and the permeability of ethidium bromide into vaccinia virus was increased due to the electrical lysis.

SEM images of particles and traces After the lysis experiment, the surface of the device was observed with SEM to ensure the electrical lysis of the vaccinia virus. Figure 4 shows the various particles found on the chip surface, near the probe array. Figure 4(a), shows a vaccinia virus particle, which has the size of 200~300 nm and the characteristic rounded brick shape. Although the particle is largely intact and undamaged, the thin line and the fragment of the outer layer can be observed, suggesting the partial damage on the viral particle. Figure 4(b) presents fully lysed vaccinia particle, showing inter-cellular tubules with 30 nm diameter. The similar tubules were also observed with a chemical lysis study of vaccinia virus (Malkin et al. 2003). Figure 4(c) shows the fragment of the tubules, discovered on the device surface.

In addition, the traces of DNA were found on the chip surface, as shown in Fig. 5(a and b). The width of these traces ranges from 50 to 200 nm. Some of these traces can be found in the fluorescence images of the device surface, as can be seen in Fig. 5(c and d). These fluorescence images were taken directly after removing the PDMS cover. The DNA was previously extracted form the viral core by strong electric field and got stained with ethidium bromide in fluidic channel. The images were pseudo-colored for clear comparison. The two patterns from SEM images and fluorescence images were located at the same spot and they

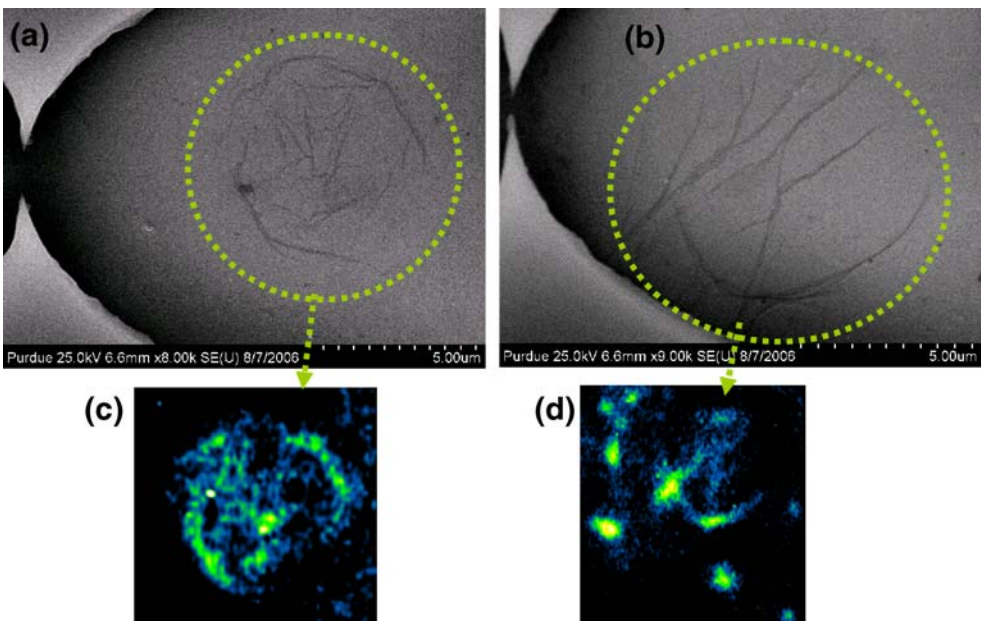

Fig. 5 (**a**, **b**) show the SEM images of DNA found on the device surface. (**c**, **d**) show the fluorescence (ethidium bromide) images of the same area of the device. The fluorescence images were taken directly after removing the PDMS cover

were very consistent to each other. Thus, it can also be concluded that those traces are produced by the viral DNA extracted from the vaccinia particles, which also proves the lysis of the vaccinia virus particle.

4 Conclusion

In this study, a nanoscale probe array for capture and lysis of viral particles was integrated into a microfluidic channel. Simple dry etch process and repeated oxidations were used to fabricate the probe array. The dielectrophoresis force produced by the probe array was strong enough to capture a vaccinia virus from the fluid and, with the same probe array the electrical lysis of the captured vaccinia virus was performed without any reagents. The damaged virus particles and DNA traces on chip surfaces were found on the device surface, as confirmed with the SEM images. This nanoscale probe array can be easily integrated with subsequent analysis modules, which can analyze single or a few number of immobilized particles captured with positive dielectrophoresis, or extracted intracellular materials, such as DNA or proteins without lytic agent.

Acknowledgment This material is based upon work supported by the National Science Foundation under Grant No. ECCS-0404107 (NSF NER) and EEC-0425626 (NSF NSEC at OSU) which supported Kidong Park. Demir Akin was supported by NIH/NIBIB Grant R21/R33EB00778-01.

References

D. Akin, H. Li, R. Bashir, Nano Lett. **4**, 257 (2004)
S. Bourland, J. Denton, A. Ikram, G.W. Neudeck, R. Bashir, J. Vac. Sci. Technol. B. **19**, 1995 (2001)
D.D. Carlo, K. Jeong, L.P. Lee, Lab Chip **3**, 287 (2003)
K.L. Chan, P.R.C. Gascoyne, F.F. Becker, R. Pethig, Biochm. Biophys. Acta. **1349**, 182 (1997)
C.F. Chou, F. Zenhausern, IEEE Eng. Med. Biol. Mag. **22**, 62 (2003)
R.C. Condit, N. Moussatche, P. Traktman, Adv Virus Res. **66**, 31 (2006)
M. Cyrklaff, C. Risco, J.J. Fernández, M.V. Jiménez, M. Esteban, W. Baumeister, J.L. Carrascosa, Proc. Natl. Acad. Sci. USA **102**, 2772 (2005)
A. Ghafoor, D. Akin, R. Bashir, Nanobiotechnology **1**, 337 (2006)
F. Grom, J. Kentsch, T. Müller, T. Schnelle, M. Stelzle, Electrophoresis **27**, 1386 (2006)
M.P. Hughes, H. Morgan, F.J. Rixon, Biochim Biophys Acta **1571**, 1 (2002)
M.P. Hughes, H. Morgan, J. Phys. D: Appl. Phys. **31**, 2205 (1998)
D.W. Lee, Y.H. Cho, MEMS 2006, (Istanbul, 2006), p. 426
S.W. Lee, Y.C. Tai, Sens. Actuators, A-Physical, **73**, 74 (1999)
T.J. Lewis, IEEE Trans. Dielectr. Electr. Insul. **10**, 769 (2003)
R.H. Lie, J. Yang, R. Lenigk, J. Bonanno, P. Grodzinski, Anal. Chem. **76**, 1824 (2004)
H. Lu, M.A. Schmidt, K.F. Jensen, Lab Chip **5**, 23 (2005)
A.J. Malkin, A. McPherson, P.D. Gershon, J. Viol. **77**, 6332 (2003)
T.S. Ravi, R.B. Marcus, D. Liu, J. Vac. Sci. Technol. B **9**, 2733 (1991)
H.Y. Wang, A.K. Bhunia, C. Lu, Biosens. Bioelectron. **22**, 582 (2006)
L.C. Waters, S.C. Jacobson, N. Kroutchinina, J. Khandurina, R.S. Foote, J.M. Ramsey, Anal. Chem. **70**, 158 (1998)
L. Yobas, W. Hui, H. Ji, Y. Chen, S. Liw, J. Li, C.S. Chong, X. Ling, C.K. Heng, H.J. Lye, S.R. Bte, K. Lee, S. Swarup, S.M. Wong, T.M. Lim, Sensors 2005, (Irvine, 2005), p 49